Chapter 7

Comparison of Pollination Graphs

James H. Lee, David M. Chan and Rodney J. Dyer

Additional information is available at the end of the chapter

http://dx.doi.org/10.5772/intechopen.74553

Abstract

From the agent-based, correlated random walk model presented, we observe the effects of varying the maximum turning angle, $\delta_{\max}$, tree density, ω, and pollen carryover, κ_{max}, on the distribution of pollen within a tree population by examining pollination graphs. Varying maximum turning angle and pollen carryover alters the dispersal of pollen, which affects many measures of connectivity of the pollination graph. Among these measures the clustering coefficient of fathers is largest when $\delta_{\max}$ is between 60 and 90°. The greatest effect of varying ω is not on the clustering coefficient of fathers, but on the other measures of genetic diversity. In particular when comparing simulations with randomly placed trees with that of actual tree placement of *C. florida* at the VCU Rice Center, it is clear that having specific tree locations is crucial in determining the properties of a pollination graph.

Keywords: pollination network, correlated random walk, agent-based model, pollen carryover, tree density

1. Introduction

While the movement of genes from one generation to the next ensures the cohesiveness of plant species through time and space [1–3], the extent to which individual sites and populations are functionally connected is mitigated by both biotic and abiotic factors [4]. For wind dispersed pollen, features such as the direction and speed of the wind and physical properties of individual pollen grains [5] play prominent roles in how genes are carried across the landscape. In addition to intrinsic factors, site-specific features, such as the structural

complexity of the landscape and co-occurring species [6], also influence connectivity to an extent that it is easy to discern.

Genes that are dispersed via active agents—animal mediated pollination—add increasing layers of involvement for at least two reasons. First, the way in which an animal disperser identifies, perceives, and interacts with features in the environment directly impact realized genetic connectivity. Over the last decade, enough work has been focused on this topic to denote a new subdiscipline of population genetic research, dubbed landscape genetics [7, 8], has been is devoted to developing methods for this task. From the perspective of the plant population, the characteristics of the intervening landscape determine the overall *porosity* of the landscape. Second, while the determination of which subset of features is important as it specifies the matrix through which pollinators move, the consequences to plant population genetic structure from alternative modes of pollinator movement is largely unexplored—even for the same plant species, alternative pollinating species leave discernibly distinct genetic structure [4, 9].

In this manuscript, we examine how the way in which pollinating individuals move across the landscape may influences population genetic structure. Here we develop an agent-based model (ABM) to simulate pollinator movement across a spatially explicit landscape. Individual pollinators are tracked as they pick up and disperse pollen among a set of individual plants. We adopt an underlying model of a correlated random walk (CRW) [10], where the direction and rate of movement is both temporally autocorrelated, though constrained. Within this framework, we explore the extent to which the spatial arrangement of trees interacts with variation in model parameters in producing variation in pollination statistics. We then apply this model to a data set from an natural population of the understory tree, *Cornus florida* L. (Cornaceae) [11]. This data set consists of both spatial and genetic information upon which previous landscape genetic studies have been conducted [11].

2. Background and methods

The agent based model developed herein uses two different categories of actors; trees act as the source and destination of pollen, and pollinating agents move individual pollen grains across the landscape. While the *trees* are spatially fixed on the landscape, the movement characteristics of the pollinating agents determine the ability of the plant population to maintain population genetic structure and determine relative reproductive output for individual trees. The movement of pollinating agents across the landscape is defined as a correlated random walk parameterized by inertia and speed. Across model runs, the aggregate movements of pollinating agents define a *de facto* pollination network whose characteristics are used to infer the robustness of the overall mating network and provide insights into population genetic stability. Across replicate runs, we extract parameters describing pollinator-movement dynamics parameters (average and maximum dispersal distances), pollen network robustness (pollen donor connectance and spatial clustering), and future population genetic structure (pollen donor density and diversity).

2.1. Field characteristics

The field size for model runs is set as a square 100×100 units grid. The density of the trees simulated on this landscape, ω, is determined as

$$\omega = \frac{\tau}{100 \times 100} = \frac{\tau}{10,000} = 0.0001\tau, \tag{1}$$

where τ is the number of trees. In our simulation runs, we used tree densities, measured in trees per square unit, of $\omega \in \{0.0250, 0.0500, 0.0750, 0.1000, 0.1500\}$.

Previous simulation and empirical work has shown that density of pollen donors can have significant impacts on the genetic structure and diversity of offspring [6, 12], and as such should be a parameter across which we evaluate the other features of this model. The simulation field has rigid boundaries, and is considered impermeable. As such pollinators cannot leave the field nor are new pollinators allowed to enter the field during a model run. When an pollinator comes into contact with the edge of the field, its subsequent heading is set such that it 'bounces' off of the barrier at the opposite angle from which it approached.

Simulations were also run for a field size of $\frac{3100}{\sqrt{541}} \times \frac{1100}{\sqrt{541}} \approx 133.2794 \times 47.2927$ units. This was used based on data for trees sampled from the experimental natural population at the Virginia Commonwealth University, Rice Rivers Center (http://ricerivers.vcu.edu). This population was used as it has been the focus of previous work on pollen-mediated gene flow [11]. The tree density that results from this data set was $\omega = 0.071552$ trees per square unit, which was also simulated as a uniformly distributed scenario along with others previously mentioned.

2.2. Tree characteristics

For tracking purposes, each tree, T, is numbered such that $1 \leq T \leq \tau$. Let $\mathbf{Y}^{(T)} = \left(y_1^{(T)},\ y_2^{(T)}\right)$ be the location of tree T, which is static. For the initial model runs, trees are randomly placed using a uniform random distribution within the allotted field size. For both simplicity and comparison to temperate tree species, we assume that all trees are self-incompatible and that all successful pollination and fertilization produces non-inbred individuals. This means that all pollination distances will be strictly greater than zero since at most one tree can occupy any location on the landscape. We also applied the model to a spatial arrangement of trees mimicking a natural population for which we have already conducted extensive empirical studies of insect-mediated pollination and gene flow. To create the pollination graph, data was collected to determine the number of seeds fertilized on each tree, which pollen donor trees are sired those seeds, and the frequency each tree fathered seeds on other trees.

For the second part of the study, coordinates of the trees at the VCU Rice Center were provided by the Dyer Laboratory [13]. These coordinates were used to create pollination graphs to compare with the random location pollination graphs to gauge the extent to which spatial heterogeneity influences broad trends in pollen connectivity.

2.3. Pollinator movement

Both natural and managed landscapes contain a broad range of species that are commonly distributed with a high degree of spatial heterogeneity. For tree species, reproductive structures may be nestled among several other taxa both below and above the target species in a mixed forest canopy. Under these conditions, a movement model based upon correlated random walk is preferred over alternatives such as Levy walks due to the complexity of the intervening landscape and the lack of long thoroughfares in the forest. Correlated Random Walk (CRW) models have been widely used to describe foraging behavior across a range of animal taxa [14–18].

In our simulations, we begin with an allotment of 1000 pollinators starting at random location with a random direction of travel on the simulated landscape. At each discrete time step, each pollinating agents will obtain a new heading based upon its previous heading with a specified random deviance. The individual will then move in this new direction 1 distance unit. This process continued for n_{max} time steps.

If a pollinator is within one unit distance of a tree, it will visit flowers on the tree. Each flower on a tree can be pollinated with equal probability. Pollinators visit one tree at a time. If multiple trees are within 1 unit the closest one is chosen. When visiting a tree, the pollinator may both gather pollen and deposit pollen from other trees. Due to the short length of the simulation we assume there are a sufficient number of flowers to gather pollen from and deposit pollen to on each tree.

Let β be the total number of pollinators in a simulation, and let $\mathbf{X}_n^{(i)} = \left(x_{1,n}^{(i)},\ x_{2,n}^{(i)}\right)$ be the location of the i^{th} pollinator, $1 \le i \le \beta$, at time step n, $0 \le n \le n_{\max}$. For all simulations, we assume $\beta = 1000$ and $n_{max} = 600$.

The initial position of each pollinator, $\mathbf{X}_0^{(i)}$ is uniformly distributed throughout the field. Each pollinator's initial heading, $-180^\circ \le \theta_1^{(i)} \le 180^\circ$ is chosen from a uniform random distribution. At each subsequent time step, the pollinator's new heading $\theta_{n+1}^{(i)}$ is dependent upon its current heading $\theta_n^{(i)}$ and a random number $\delta_{n+1}^{(i)}$. That is

$$\theta_{n+1}^{(i)} = \theta_n^{(i)} + \delta_{n+1}^{(i)} \tag{2}$$

where $\delta_{n+1}^{(i)} \in (-\delta_{\max},\ \delta_{\max})$ for each $n = 1,\ \ldots,\ n_{\max}$. Similarly, the initial step size of each pollinator, $r_1^{(i)} = 1$ at time $n = 1$. Each subsequent step size, $r_{n+1}^{(i)} \in (0,\ r_{\max})$ uniformly distributed for each $n = 1,\ \ldots,\ n_{\max}$. In Cartesian coordinates, the position of the i^{th} pollinator at each subsequent time step will be

$$\mathbf{X}_{n+1}^{(i)}\left(\mathbf{X}_n^{(i)};\ r_{n+1}^{(i)},\ \theta_{n+1}^{(i)}\right) = \left(x_{1,n}^{(i)} + r_{n+1}^{(i)}\cos\left(\theta_{n+1}^{(i)}\right),\ x_{2,n}^{(i)} + r_{n+1}^{(i)}\sin\left(\theta_{n+1}^{(i)}\right)\right) \tag{3}$$

for each $n = 1,\ \ldots,\ n_{\max}$. In our simulations we used values of $\delta_{\max} \in \{0^\circ, 15^\circ, 30^\circ, 45^\circ, 60^\circ, 75^\circ, 90^\circ, 120^\circ, 150^\circ, 180^\circ\}$.

Sample paths based on different values of δ_{max} are shown in **Figure 1**. As δ_{max} increases the paths do not generally travel away as far from the starting point and loop around more often. A path with $\delta_{max} = 0$ would be along a straight line, which is not shown here.

2.4. Pollination

If a pollinator visits a flower, it will collect pollen from that individual. Pollen will be deposited with a probability of P_κ, where κ is the number of previously visited flowers, to account for pollen carryover. Carryover probability $P_\kappa = 0$ if $\kappa > \kappa_{\max}$ where $\kappa_{\max}$ is the maximum pollen carryover. In the simulations the pollination carryovers used were $\kappa_{\max} \in \{1, 3, 5, 7, \infty\}$.

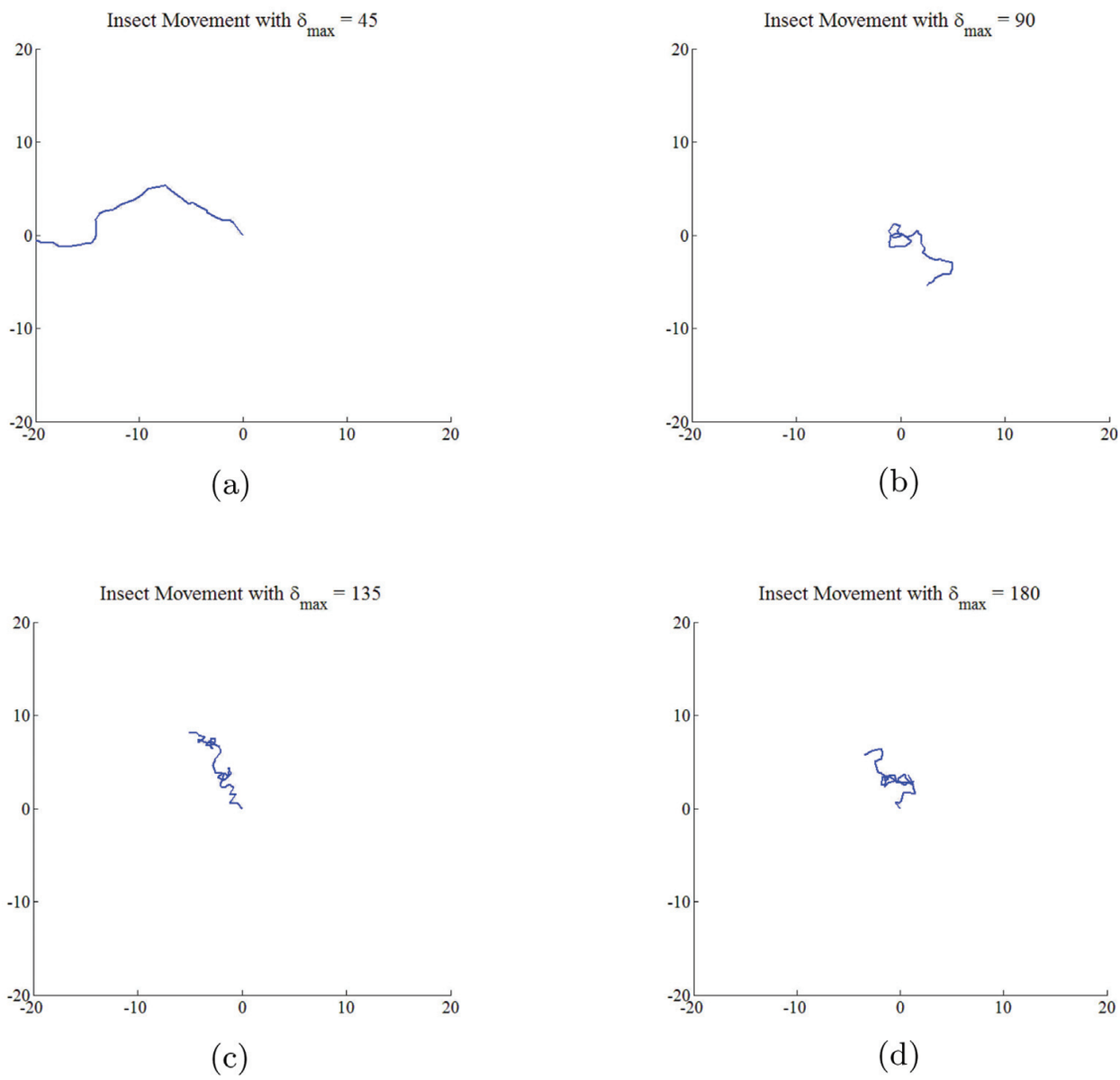

Figure 1. Sample paths based on δ_{max}.

As a pollinator visits multiple flowers, the chances that it deposits pollen from a previous flower diminishes with each successive flower visited [19]. It was shown by [20] that from a given flower, a pollinator will deposit roughly $\gamma(1-\gamma)^{k-1}$ pollen grains onto the k^{th} flower visited, where γ depends upon the type of pollen as well as the type of pollinator. In this study, the probability that an pollinator distributes pollen from one tree to another tree is given by

$$P_\kappa = \begin{cases} \rho(1-\rho)^{\kappa-1} & \text{if } \kappa \le \kappa_{\max} \\ 0 & \text{otherwise} \end{cases} \tag{4}$$

where κ is the number of previously visited flowers, and ρ is the chance of pollination when $\kappa = 1$. For the simulation work we used $\rho = 0.30$ based on work by [21].

2.5. Statistics

To characterize pollen movement and how it responds to the parameters of the models, pollination graphs were constructed. The connectivity network is based upon the physical location of individual trees and the pattern of spatial pollen movement created by the pollinators. In this network, each tree is represented as a node and the edges designate the movement of pollen from donor (paternal individual) to recipient (maternal individual), creating a directed pollination graph.

The parameters we vary in constructing these networks include tree density, ω, pollination carryover, κ, and pollinator maximum turning angle, $\delta_{\max}$. To determine the effect of these parameters on the landscape pattern of connectivity, we estimated the *number of fathers per mother*, Φ_m, *connectance*, L, *average weighted diversity of fathers*, E, *average pollination distance*, $\overline{D}$, *average maximum pollination distance*, $\tilde{D}$, and the *weak and strong clustering coefficients of fathers*, C_{weak} and C_{strong}.

Each tree has the ability to contribute pollen to other trees and to accept pollen from other trees. When applicable, we will refer to a tree as a father tree, f, if that tree contributes pollen to another tree. We will refer to a tree as a mother tree, m, if that tree is accepts pollen from another tree. Let ϕ_m be the set of trees which father seeds on tree m, then the number of fathers for each tree m in the graph is $|\phi_m|$, $m = 1, 2, \ldots, \tau$, where $|\cdot|$ denotes cardinality. The set containing the *number of fathers per mother* for all trees in the graph is

$$\Phi_m = \{|\phi_1|, |\phi_2|, \ldots, |\phi_\tau|\}. \tag{5}$$

This value is similar to the degree distribution in the studies by Ramos-Jilberto et al. [22] and Valdovions et al. [23].

From this construct, we then create the $\tau \times \tau$ adjacency matrix, $\mathbf{A} = [a_{i,j}]$, where $a_{f,m} = 1$ if tree f fathers at least one seed on tree m, and 0 if not. Thus $\mathbf{A}$ is a binary representation of the connectance of the graph. Since the trees do not self-pollinate, the number of possible interactions on this matrix is $\tau(\tau - 1)$.

The *connectance*, L, of a graph is defined as the proportion of realized pollination events to the number of possible pollination events [24]. The connectance of the graph is given by

$$L = \frac{\sum_{f=1}^{\tau} \sum_{m=1}^{\tau} a_{f,m}}{\tau(\tau - 1)}. \tag{6}$$

As with the previous parameters, connectance has been used in a number of settings, see [23, 25–28], where the graphs is between species. In this study the focus is on individuals, and so the connectance is the proportion of realized pollination events between individual plants.

Furthermore, if there is an edge between tree m and tree f where tree $f \in \phi_m$, then denote $b_{f,m}$ to be the weight of that edge, which is equal to the number of times tree f fathers seeds on tree m. With this we create the matrix $\mathbf{B} = \left[b_{i,j}\right]$, which is a $\tau \times \tau$ matrix such that $b_{f,m}$ is the number of seeds that tree f fathers on tree m. The weighted diversity of fathers for a mother tree m is a weighted measurement of the number of fathers that contribute pollen to seeds on m, accounting for the various number of seeds fathered by each father tree. The weighted diversity of fathers, $\widehat{F}_m$, is computed for each m in the graph by the formula

$$\widehat{F}_m = \frac{\left(\sum_{f=1}^{|\phi_m|} b_{f,m}\right)^2}{\sum_{f=1}^{|\phi_m|} \left(b_{f,m}\right)^2}. \tag{7}$$

The *average weighted diversity of fathers* is the mean average of the weighted diversity of fathers over all mother trees, and is given by the formula

$$E = \frac{1}{\mu} \sum_{m=1}^{\mu} \widehat{F}_m, \tag{8}$$

where $0 \leq \mu \leq \tau$ is the total number individuals in the graph.

The average pollination distance for an pollinator i is the average of the distances between any two trees mated by i. Let $\mathbf{Y}^{(f^{(i)})} = \left(y_1^{(f^{(i)})}, \; y_2^{(f^{(i)})}\right)$ be the location of father tree $f^{(i)}$ and $\mathbf{Y}^{(m^{(i)})} = \left(y_1^{(m^{(i)})}, \; y_2^{(m^{(i)})}\right)$ be the location of mother tree $m^{(i)}$ where pollinator i delivers pollen from tree $f^{(i)}$ to tree $m^{(i)}$. Then the average pollination distance, $\overline{D}^{(i)}$, achieved by pollinator i for all such pairings is

$$\overline{D}^{(i)} = \frac{1}{\mu^{(i)}} \sum_{m=1}^{\mu^{(i)}} \sum_{f=1}^{\phi_m^{(i)}} \frac{1}{\phi_m^{(i)}} \sqrt{\left(y_1^{(m^{(i)})} - y_1^{(f^{(i)})}\right)^2 + \left(y_2^{(m^{(i)})} - y_2^{(f^{(i)})}\right)^2}, \tag{9}$$

where $\mu^{(i)}$ is the number of mother trees pollinated by pollinator i, and ϕ_m^i are the number of father trees pollinating tree m by pollinator i. The average pollination distance, $\overline{D}^{(i)}$, for each

pollinator is averaged over the total number of pollinators, β, to obtain the *average pollination distance*, $\overline{D}$, for the graph

$$\overline{D} = \frac{1}{\beta} \sum_{i=1}^{\beta} \overline{D}^{(i)}. \tag{10}$$

The *maximum pollination distance* for an pollinator i is

$$\tilde{D}^{(i)} = \max_{m^{(i)} \le \mu^{(i)},\ f^{(i)} \le \phi_m^{(i)}} \left(\sqrt{\left(y_1^{(m^{(i)})} - y_1^{(f^{(i)})} \right)^2 + \left(y_2^{(m^{(i)})} - y_2^{(f^{(i)})} \right)^2} \right). \tag{11}$$

The maximum pollination distance for each pollinator is averaged over all of the pollinators to obtain the *average maximum pollination distance* for the graph

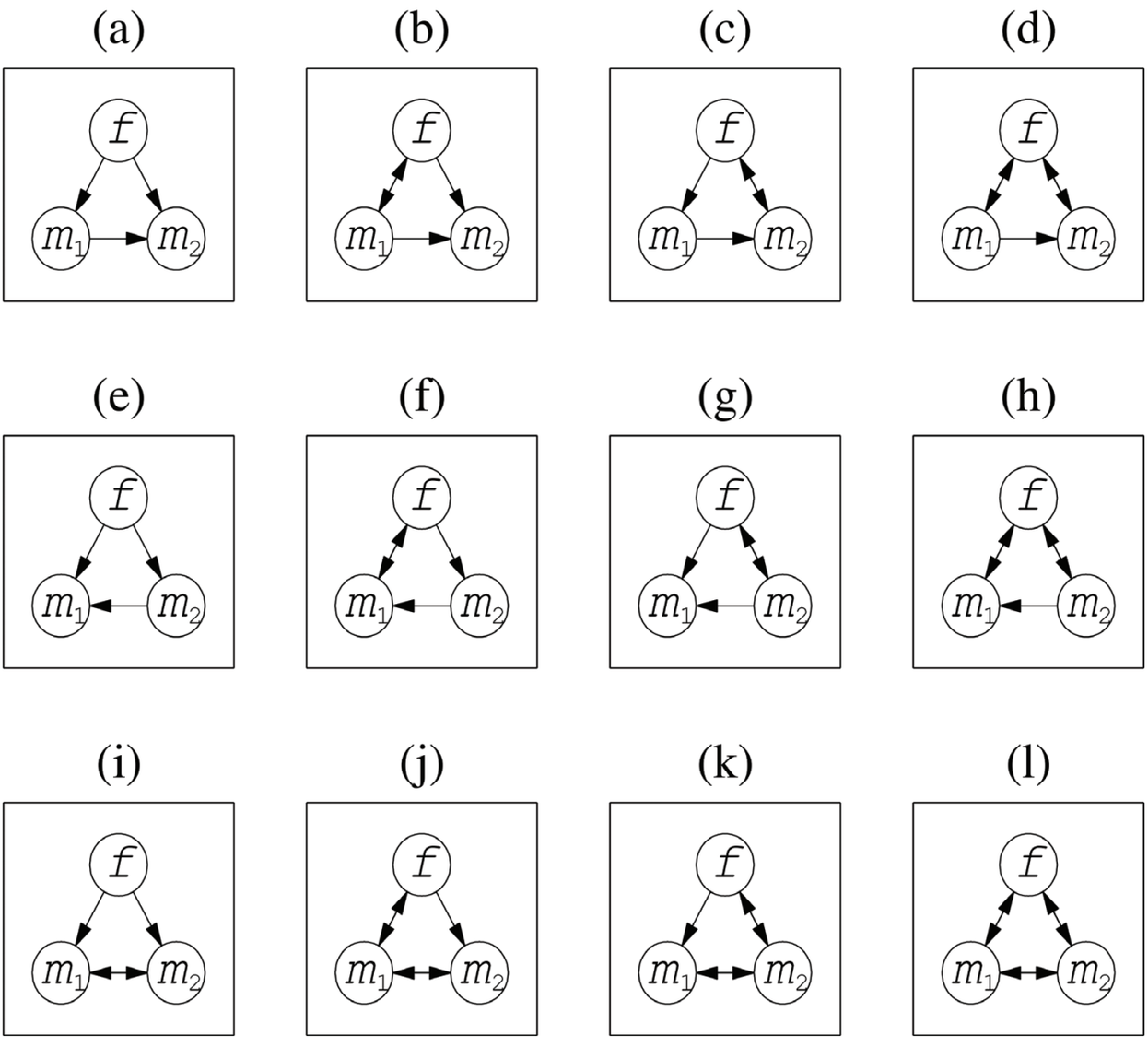

Figure 2. Fathering triangles. Arrows indicate direction of gene flow.

$$\tilde{D} = \frac{1}{\beta} \sum_{i=1}^{\beta} \tilde{D}^{(i)}. \tag{12}$$

A fathering triplet is the relationship between three trees such that tree f is a father to seeds on both tree m_1 and tree m_2. These seeds are half-siblings on the paternal side. In particular a weak fathering triangle, as a subset of fathering triplets, is one such that m_1 also fathers seeds on m_2 (**Figure 2(a)–(d)**), m_2 fathers seeds on m_1 (**Figure 2(e)–(h)**), or both (**Figure 2(i)–(l)**). A strong fathering triangle is defined as fathering triangle where f, m_1, and m_2 all father seeds on each other (**Figure 2(l)**).

The *weak clustering coefficient of fathers*, C_{weak}, is the number of weak fathering triangles in the pollination graph over the total number of fathering triplets

$$C_{\text{weak}} = \frac{\text{number of weak fathering triangles}}{\text{number of fathering triplets}}. \tag{13}$$

The *strong clustering coefficient of fathers*, C_{strong} is the number of strong fathering triangles in the pollination graph over the total number of fathering triplets

$$C_{\text{strong}} = \frac{\text{number of strong fathering triangles}}{\text{number of fathering triplets}}. \tag{14}$$

C_{weak} and C_{strong} are measurements of the tendency of parent trees to be clustered together in densely connected groups.

3. Results and discussion

We examine the effect of varying parameters on the graph statistics: the number of fathers per mother, Φ_m, connectance, L, the average weighted diversity of fathers, E, the clustering coefficient of fathers, C, the average pollination distance, $\overline{D}$, and the average maximum pollination distance, $\tilde{D}$. The model was simulated a total of 10 replicate runs for each unique combination of parameters. The results follow.

3.1. Number of fathers

One way to analyze the genetic structure and connectivity within a local plant population is to examine the number of different fathers per mother tree, Φ_m. In **Figure 3**, the number of different fathers per mother in a randomized placement of trees is distributed in a Gaussian-like distribution. This is an expected outcome since gene flow should be directly proportional to the distance traveled by a pollinator. It has been shown, see [29], that the distribution range resulting from a CRW would necessarily result in Gaussian-like behavior for a large number of pollination events.

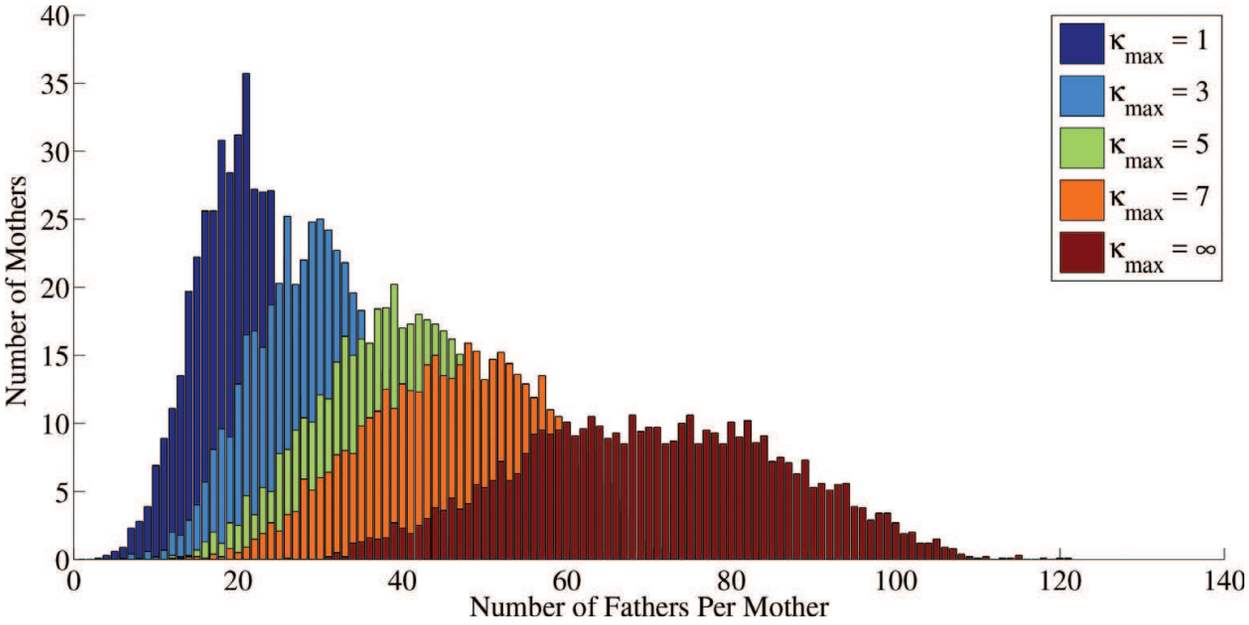

Figure 3. Number of fathers per mother. Tree density $\omega = 0.071552$ trees per square unit. Maximum pollinator turning radius $\delta_{\max} = 45^{\circ}$. Pollination chance diminishing with larger carryover. Maximum pollen carryover $\kappa_{\max} = \{1, 3, 5, 7, \infty\}$.

Of interest here is that as the maximum pollen carryover increases, the mean number of fathers increases. This is due to the increase in the variability in pollen that each pollinator can distribute, which would increase diversity. The variance in the distribution also increases as pollen carryover increases, which is also due to this increase in diversity.

However, when this distribution is compared with the tree placement at the Rice Center, see **Figure 4**, we observe a bi-modal distribution of the number of fathers per mother. This distribution

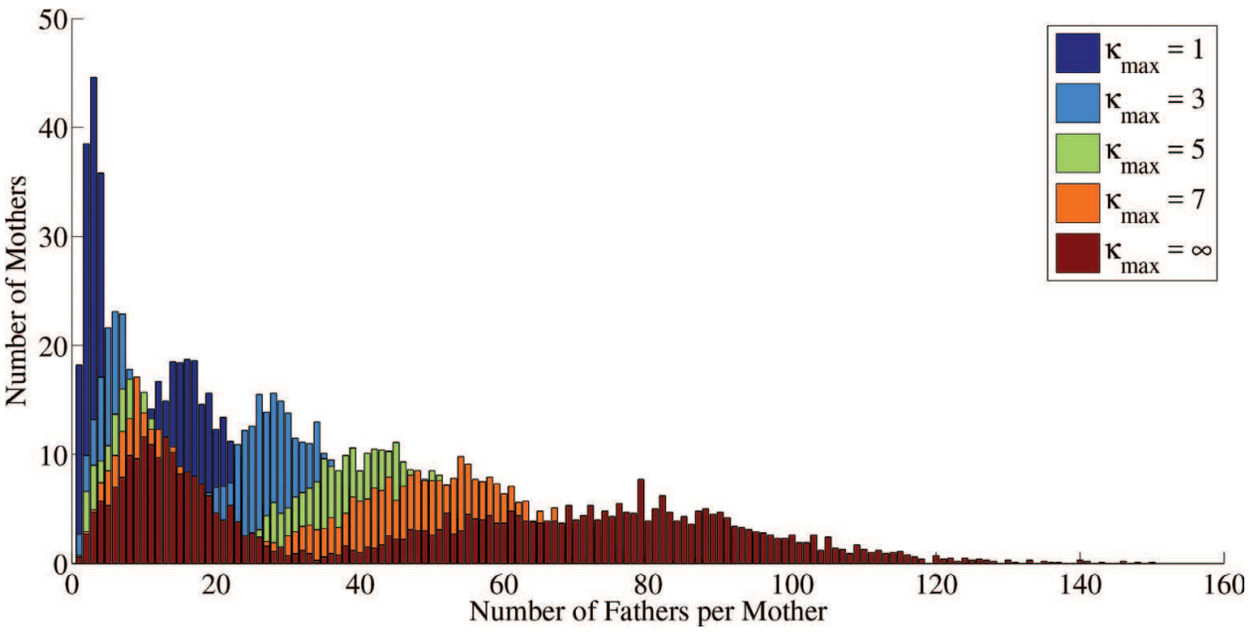

Figure 4. Number of fathers per mother. Field size 133.2794×47.2927 units. Tree density $\omega = 0.071552$ trees per square unit. Maximum pollinator turning radius $\delta_{\max} = 45^{\circ}$. Pollination chance diminishing with larger carryover. Maximum pollen carryover $\kappa_{\max} = \{1, 3, 5, 7, \infty\}$.

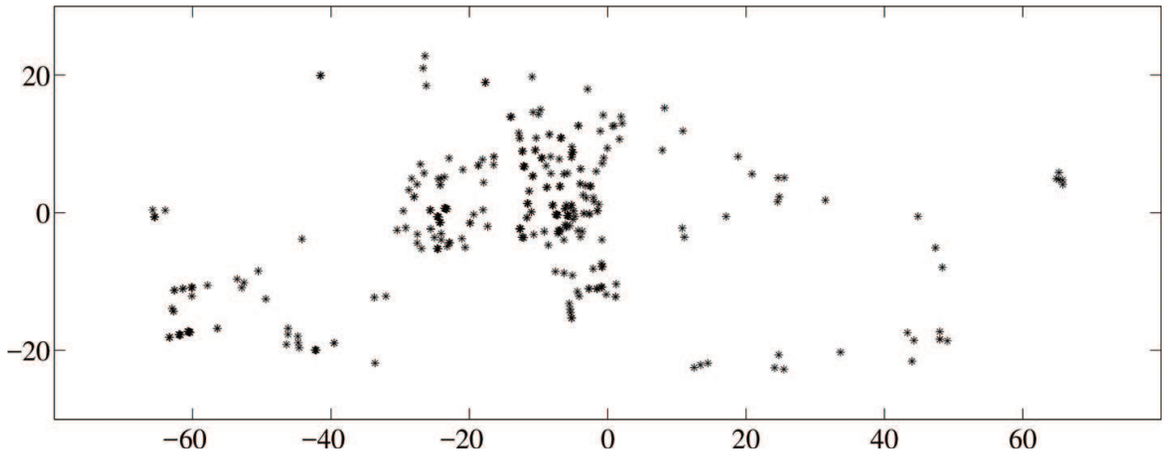

Figure 5. *Tree coordinates (scaled) at the VCU Rice Center*. Field size 133.2794×47.2927 units. Tree density $\omega = 0.071552$ trees per square units.

is attributed to the spatial heterogeneity of the research site. This influences the genetic structure and connectivity in *C. florida* populations [11] at the Rice Center.

The spatial heterogeneity is evident in **Figure 5**. The bimodal distribution of the number of fathers per mother is caused by the variation of tree density across the landscape. There is a high density group of trees in the center of the region, and the density decreases toward the boundary of the region. This region is bounded by a river and a lake on two sides, and a major road and a farm on the other two sides, which are not pictured here.

These two different density regions create the two peaks shown in **Figure 4**. In particular when $\kappa_{\max} = \infty$, the first peak is approximately 3 fathers per mother on 29 mother trees, and the second peak is 32 fathers per mother on 12 mother trees. This bimodality is present whether an pollinator is restricted to moving in a straight line, i.e., $\delta_{\max} = 0^\circ$, or with pure dispersal, i.e., $\delta_{\max} = 180^\circ$. Clearly, knowing the locations of tree is critical in understanding the gene flow in a particular area (**Figure 5**).

3.2. Connectance

The connectance is a measure of how complete a pollination graph is in terms of individuals mating with others. In **Figures 6** and **7**, we see the effect of density and maximum turning angle. With higher density, and thus more individuals, the connectance is reduced due to a much larger number of potential pairs of individuals. As the maximum turning angle increases the connectance also decreases. If an pollinator travels in a straight line, it will cover a greater spatial distance as it visits more different trees than it would if it just spun around in circles locally. Smaller $\delta_{\max}$ increases the potential for mating to occur between trees with greater distance between them. The graph connectance is three to five times greater with small $\delta_{\max}$ than it is with large $\delta_{\max}$.

If an pollinator does not venture very far from its starting location, as would be the case when $\delta_{\max}$ is close to 180°, the effect of maximum pollen carryover on the connectance of the graph decreases. When $\delta_{\max} = 0$, the connectance of the graph is nearly four times greater if the

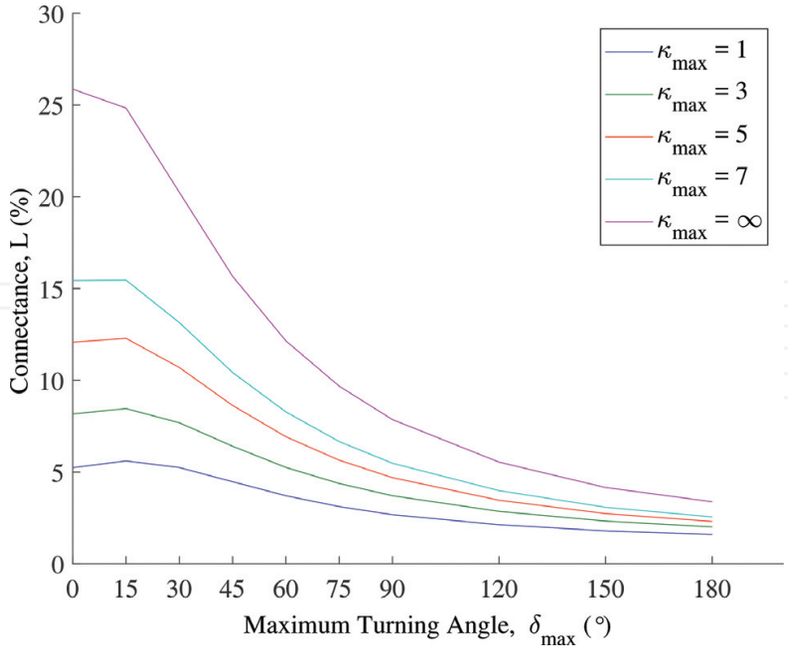

Figure 6. Connectance. Field size 133.2794 × 47.2927 units. Tree density $\omega = 0.071552$ trees per square unit. Pollination chance diminishing with larger carryover. Maximum pollen carryover $\kappa_{max} = \{1, 3, 5, 7, \infty\}$.

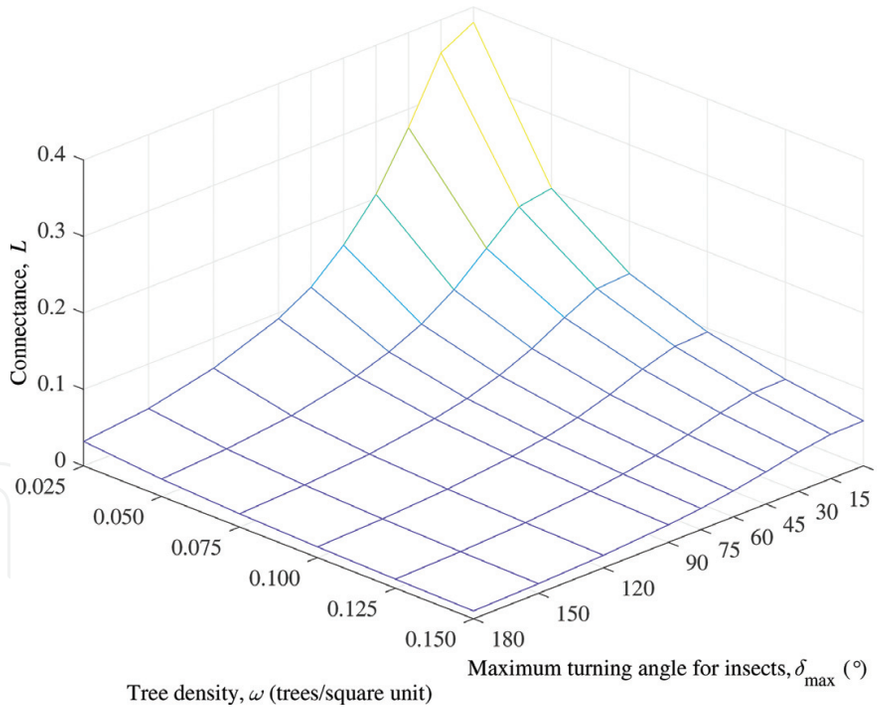

Figure 7. Connectance. Field size 100 × 100 units. Tree density in trees per square unit, $\omega = \{0.025, 0.050, 0.075, 0.100, , 0.125, 0.150\}$ ($\tau = \{250, 500, 750, 1000, 1250, 1500\}$ randomly-placed trees). Pollination chance diminishing with larger carryover. Maximum pollen carryover $\kappa_{max} = \infty$.

maximum pollen carryover is unlimited versus the case when pollen carryover is limited to only one flower. However, when $\delta_{max} = 180^{\circ}$, the connectance of the graph is only about twice if the maximum pollen carryover is unlimited.

Pollen carryover is important in connectance as well. In **Figure 7**, it is clear that if the maximum pollen carryover is limited, the connectance of the pollination graph is also limited due to the diversity of pollen an individual would have access to via the pollinator. With smaller κ_{max} the diversity of pollen distributed is greatly decreased and thus the diversity of pollination events is reduced as well.

When considering the actual tree locations at the Rice Center, the connectance of the graph is close to half of the connectance value with randomly-placed trees. The differences between the graphs is greatest when $\delta_{\max}$ is close to 0°. Connectance values for simulations run with the Rice Center data are shown in **Figure 8**.

3.3. Average weighted diversity of fathers

The average weighted diversity of fathers is clearly affected by density and the maximum turning angle, though the effects of maximum turning angle are more pronounced. In **Figure 9**, as the maximum turning angle increases, the average weighted diversity of fathers decreases. The greatest change occurs between 15 and 90° and tends to even out at the extremes. As described earlier, with greater potential for a variety of fathers, the average number of fathers contributing pollen to mother trees increases as the maximum turning angle of pollinators decreases. This adds a greater genetic diversity to the tree population. Pollinators that travel in straighter paths not only distribute pollen greater distances, but also with greater diversity. The effects of density are more pronounced at smaller maximum turning angles, where we see a reduction of the average weighted diversity of fathers as the density increases.

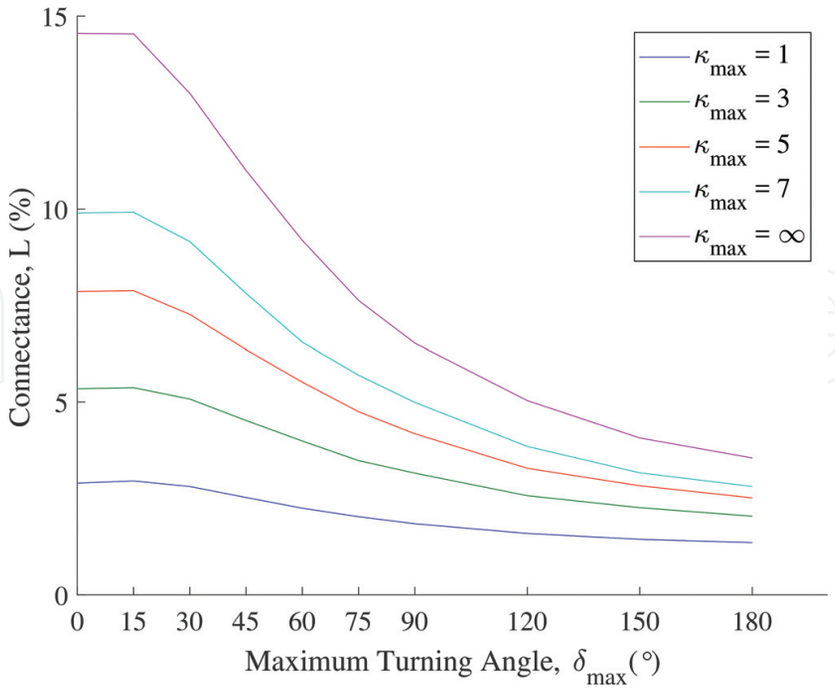

Figure 8. Connectance. Field size 133.2794×47.2927 units. Tree density $\omega = 0.071552$ trees per square unit. Pollination chance diminishing with larger carryover. Maximum pollen carryover $\kappa_{\max} = \{1, 3, 5, 7, \infty\}$.

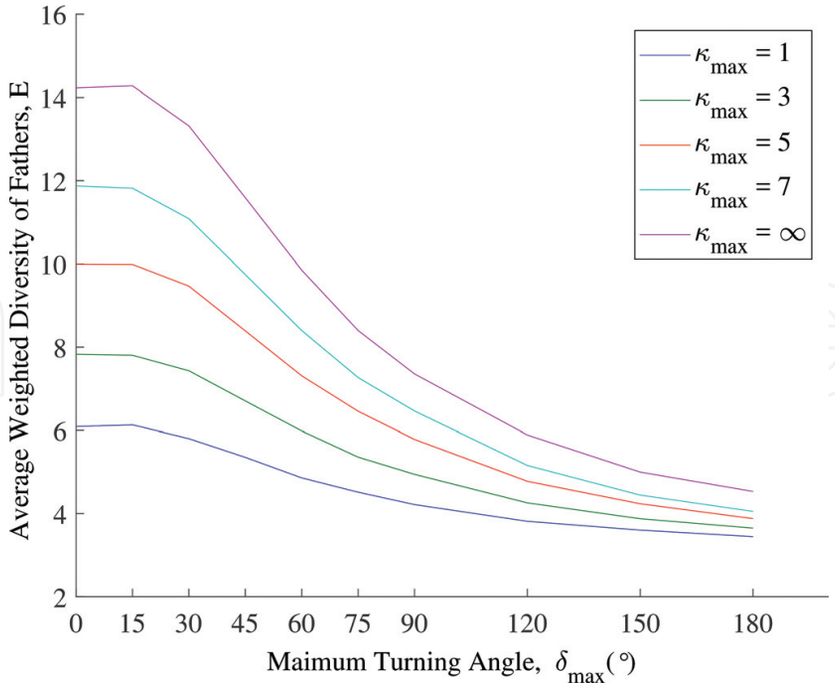

Figure 9. Average weighted diversity of fathers. Field size 100×100 units. Tree density in trees per square unit, $\omega = \{0.025, 0.050, 0.075, 0.100, 0.125, 0.150\}$ ($\tau = \{250, 500, 750, 1000, 1250, 1500\}$ randomly placed trees). Pollination chance diminishing with larger carryover. Maximum pollen carryover $\kappa_{max} = \infty$.

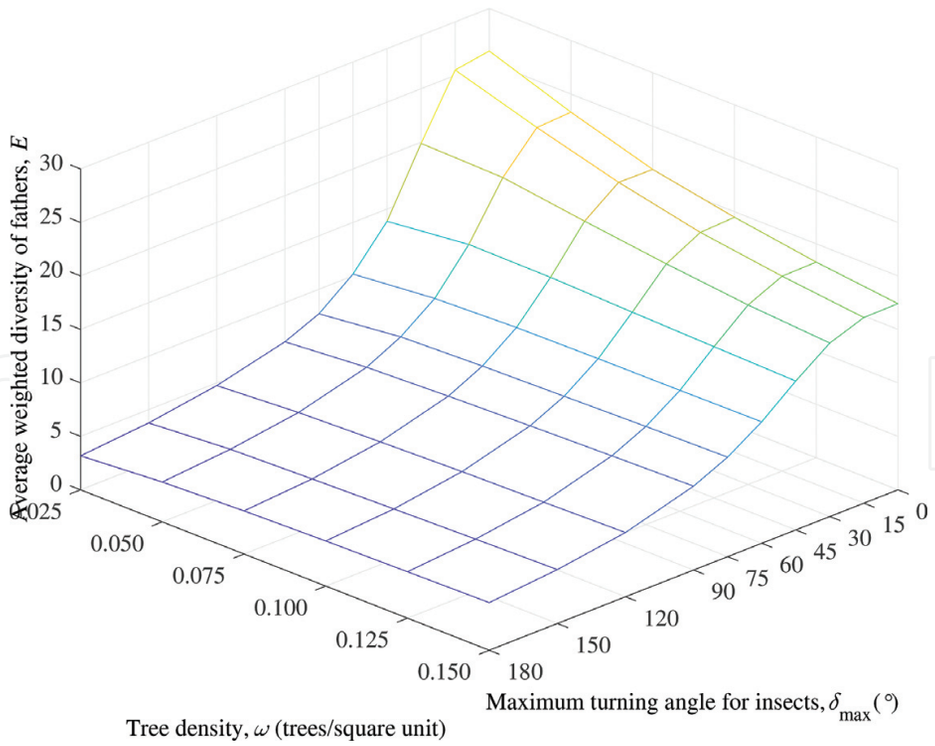

Figure 10. Average weighted diversity of fathers. Field size 133.2794×47.2927 units. Tree density in trees per square unit, $\omega = 0.071552$ ($\tau = 451$ Rice Center trees). Pollination chance diminishing with larger carryover. Maximum pollen carryover $\kappa_{max} = \{1, 3, 5, 7, \infty\}$.

The differences in average weighted diversity of fathers as pollen carryover increases are exactly as one would expect, see **Figure 10**. With higher κ_{max}, the larger the diversity in pollen increases the average weighted diversity in fathers. This increase is small for large δ_{max} due to the increase in the number of multiple visits by pollinators to the same trees.

When comparing the random tree distribution to that of the Rice Center, the random distribution has a larger average weighted diversity of fathers (not shown here) the average weighted diversity of fathers at the Rice Center is about 60% of the randomly placed trees. Trees that are in densely packed groups are going to be greatly influenced by surrounding trees, but trees at greater distances will have less of a comparative impact on the fatherhood of seeds.

3.4. Average and maximum average pollination distances

The average and maximum pollination distances behave similar to the connectance. As with the connectance, as the density increases both distances decrease, which is due to a greater number of shorter pollination events lowering the averages, see **Figures 11** and **12**. The change in density has a smaller effect on the maximum pollination distance. Also as the maximum turning angle increase both distances decreases as well since the pollinators do not travel as far. This decrease is more dramatic at lower densities.

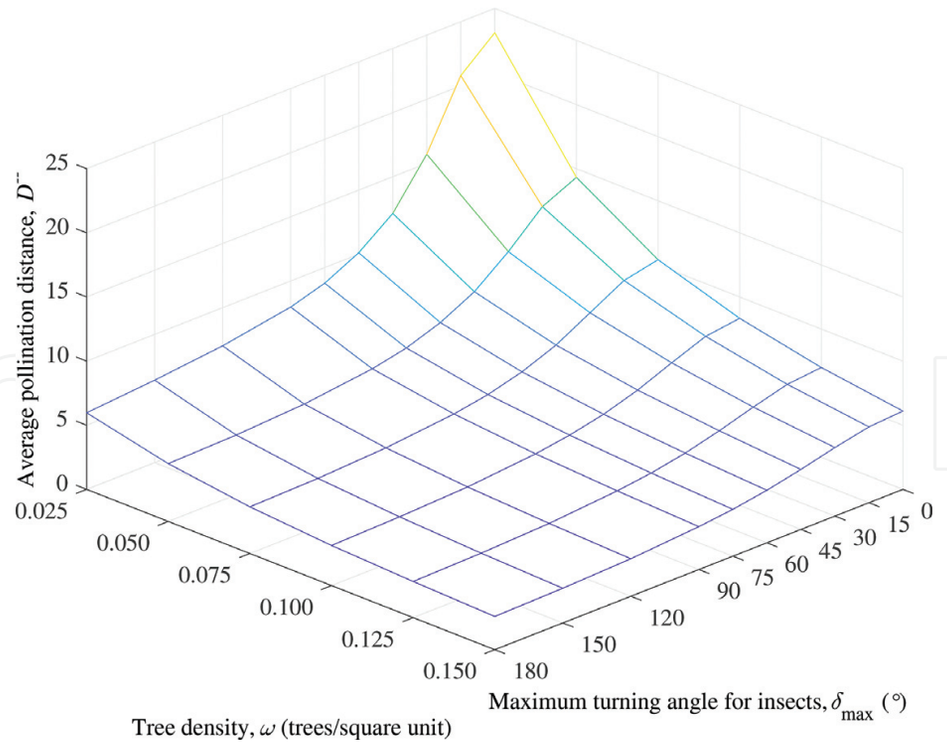

Figure 11. Average pollination distance. Field size 100×100 units. Tree density in trees per square area, $\omega = \{0.025, 0.050, 0.075, 0.100, 0.125, 0.150\}$ ($\tau = \{250, 500, 750, 1000, 1250, 1500\}$ randomly placed trees). Pollination chance diminishing with larger carryover. Maximum pollen carryover $\kappa_{\max} = \infty$.

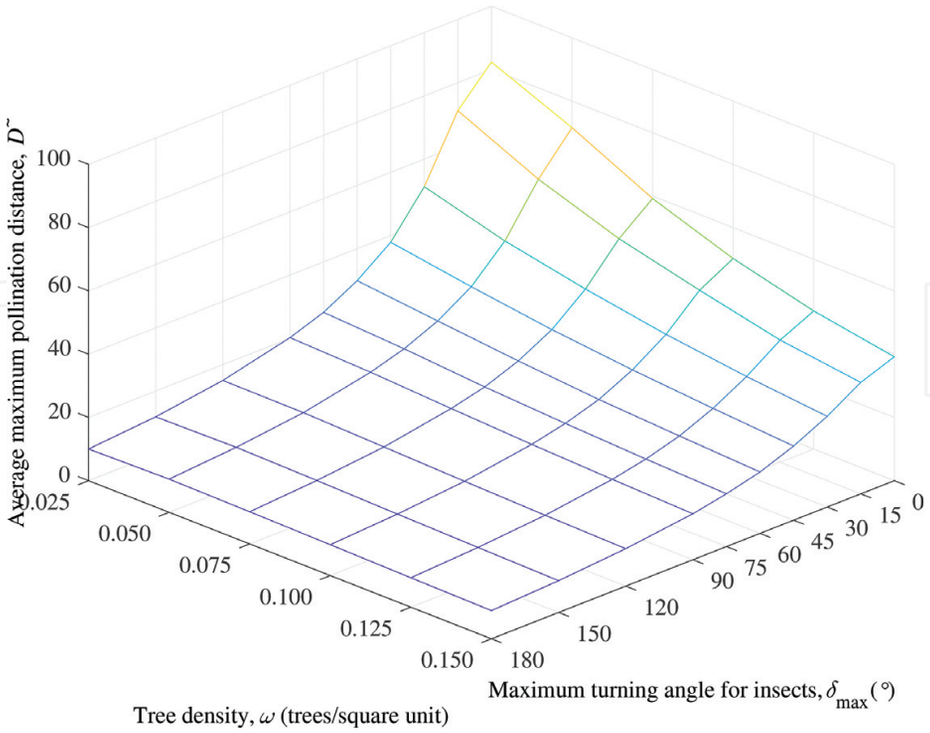

Figure 12. Average maximum pollination distance. Field size 100×100 units. Tree density in trees per square unit, $\omega = \{0.025, 0.050, 0.075, 0.100, 0.125, 0.150\}$ ($\tau = \{250, 500, 750, 1000, 1250, 1500\}$ randomly placed trees). Pollination chance diminishing with larger carryover. Maximum pollen carryover $\kappa_{max} = \infty$.

Using Rice Center locations (not shown here) if δ_{max} is close to 0°, the average pollination distance is greater than that of randomly placed trees. However, if δ_{max} is close to 180°, the average pollination distance using Rice Center data is less than that of randomly placed trees. This is again due to the combination of the low and high density distribution of trees at the Rice Center. At low δ_{max} pollinators interact with both densities of trees, whereas at high δ_{max} the interaction between these groups is greatly diminished.

We see the effects of pollen carryover in the average pollination distance is shown in **Figure 11** and in the maximum pollination distance in **Figure 12**. As expected, increasing κ_{max} increases the average pollination distance. If the pollen carryover increases that allows pollen grains to travel further since pollen can be deposited after visiting several intermediate trees.

The results are similar with the Rice Center model. The results at the Rice Center are slightly higher in distances due to the potential longer distances at the edges of the region.

3.5. Clustering coefficients of fathers

The clustering coefficient is a measure of the interconnectedness of the graph, as well as how the genes are shared within the graph. For a field of randomly placed trees, there is a maximum value for the weak clustering coefficient of fathers, C_{weak}, see **Figure 13**, that occurs between 60 and 90° for all maximum pollen carryover values, κ_{max}. This is explained by examining the extreme values of δ_{max}. For small δ_{max}, pollinators travel across the landscape

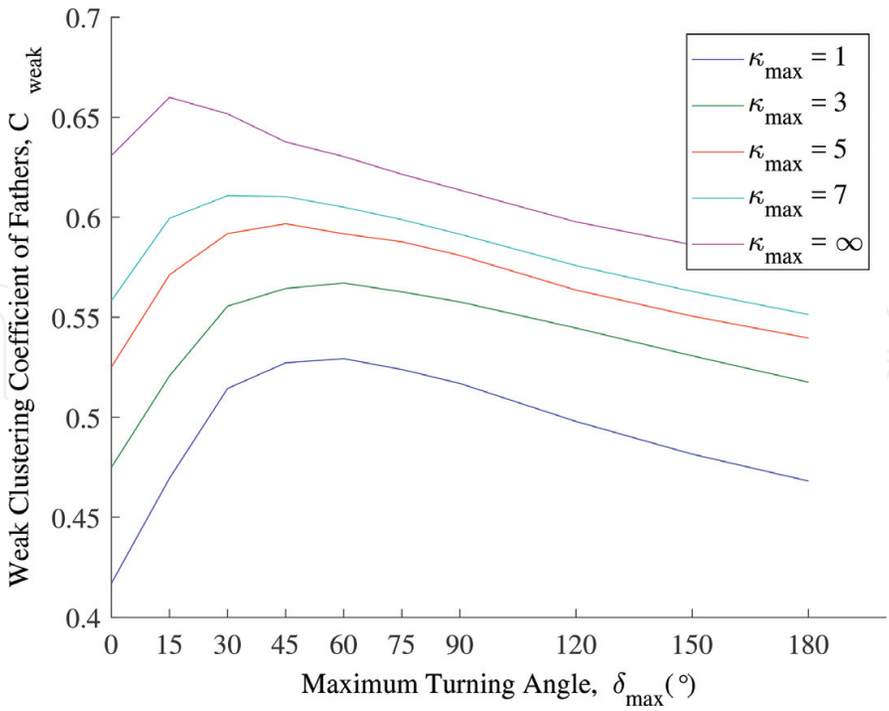

Figure 13. Weak clustering coefficient of fathers. Field size 133.2794 × 47.2927 units. Tree density $\omega = 0.071552$ trees per square unit ($\tau = 451$ randomly placed trees). Pollination chance diminishing with larger carryover. Maximum pollen carryover $\kappa_{max} = \{1, 3, 5, 7, \infty\}$.

and do not stay in a small neighborhood. Since the weak clustering coefficient of fathers is an average measure of clustering at a local level, it is natural for C_{weak} to be low if pollinators do not remain in a small neighborhood.

At the other extreme, for large δ_{max}, pollinators do not move around enough to increase the value of C_{weak}. When δ_{max} is not at an extreme value, the displacement of the pollinators is high enough to visit many trees, but low enough so more of the trees that it visits are within a closer proximity to one another.

Modeled data on the weak clustering coefficient of fathers, C_{weak}, from the Rice Center is shown in **Figure 14**. The C_{weak} values slowly increase as κ_{max} increases over the entire interval from 0 to 180°, mostly flattening out for $\kappa_{max} > 75°$. As δ_{max} approaches 180°, pollinators remain in the same general area. Thus, in locally dense patches of trees, clustering will naturally be higher.

Unexpectedly, varying the tree density, ω, did not have a major effect on C_{weak}. It would seem that varying ω would have the same quantitative effect on C_{weak} as varying the maximum pollinator turning angle, δ_{max}. We suspect that the reason for the relative consistency of values for C_{weak} is due to the having both low and high density regions. The values for C_{weak}, varying ω and δ_{max}, are shown in **Figure 15**.

Figures 16–18 are corresponding plots for strong clustering coefficient of fathers, C_{strong}. In these plots we see similar results as with the weak clustering coefficient. Numerically the C_{strong} results are a magnitude smaller than the C_{weak} results since they are a measure of a subset of possible combinations of C_{weak}. This is however a greater increase in these values with increasing density, which allows for these fathering triangles to occur.

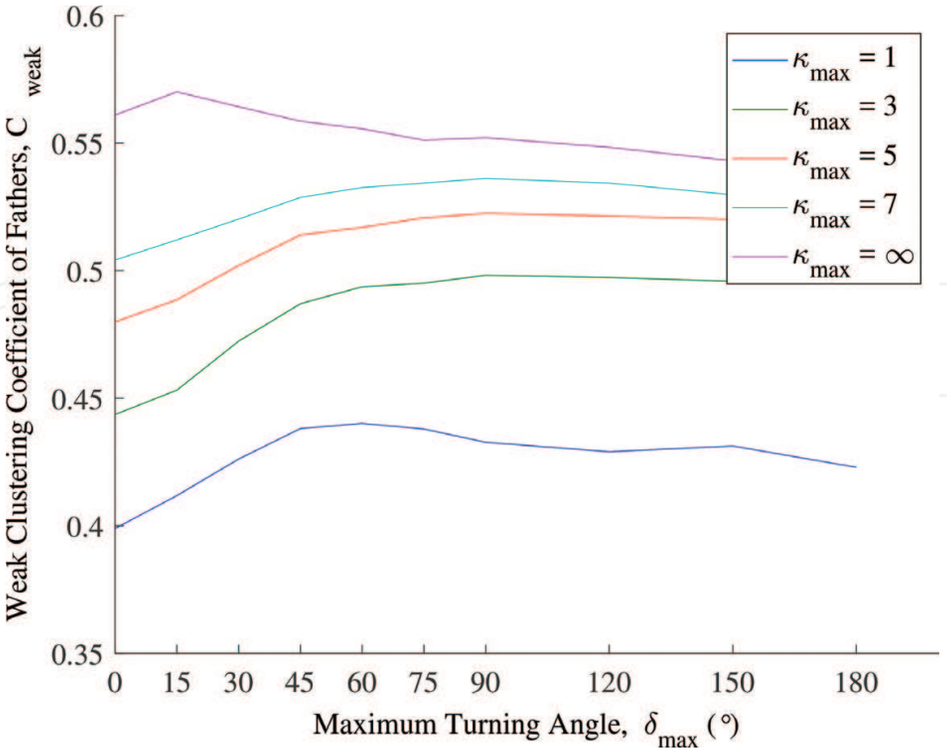

Figure 14. Weak clustering coefficient of fathers. Field size 133.2794×47.2927 units. Tree density $\omega = 0.071552$ trees per square unit ($\tau = 451$ Rice Center trees). Pollination chance diminishing with larger carryover. Maximum pollen carryover $\kappa_{\max} = \{1, 3, 5, 7, \infty\}$.

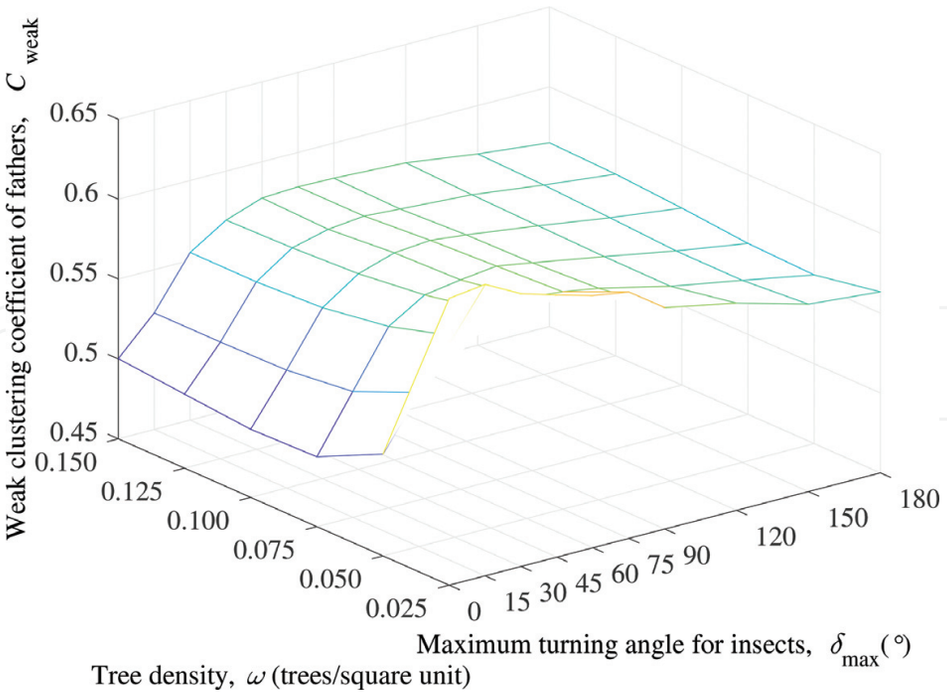

Figure 15. Weak clustering coefficient of fathers. Field size 100×100 units. Tree density in trees per square unit, $\omega = \{0.025, 0.050, 0.075, 0.100, 0.125, 0.150\}$ ($\tau = \{250, 500, 750, 1000, 1250, 1500\}$ randomly placed trees). Pollination chance diminishing with larger carryover. Maximum pollen carryover $\kappa_{\max} = \infty$.

http://dx.doi.org/10.5772/intechopen.74553

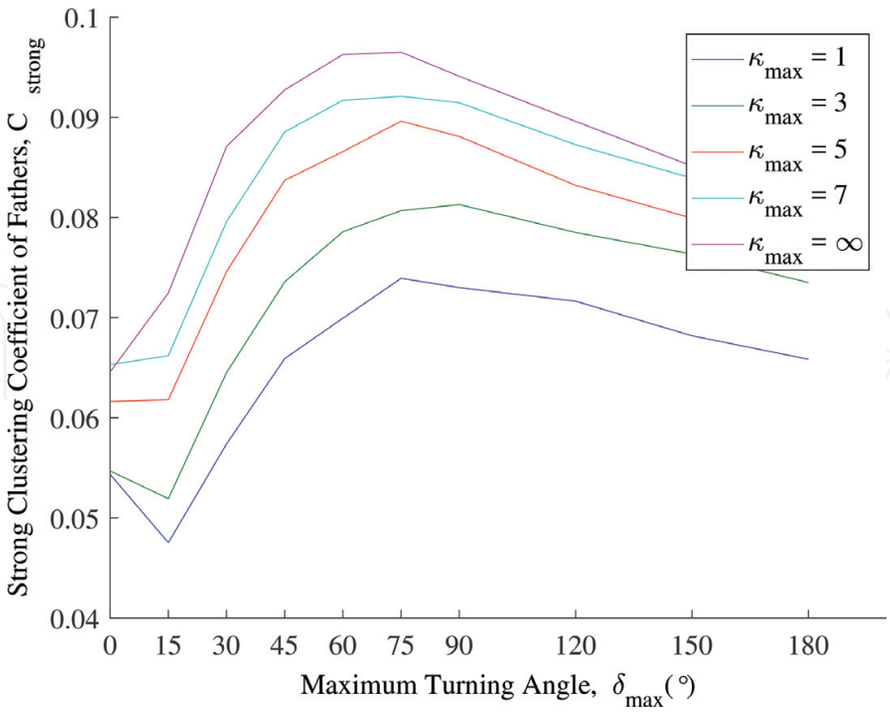

Figure 16. Strong clustering coefficient of fathers. Field size 133.2794 × 47.2927 units. Tree density $\omega = 0.071552$ trees per square unit ($\tau = 451$ randomly placed trees). Pollination chance diminishing with larger carryover. Maximum pollen carryover $\kappa_{max} = \{1, 3, 5, 7, \infty\}$.

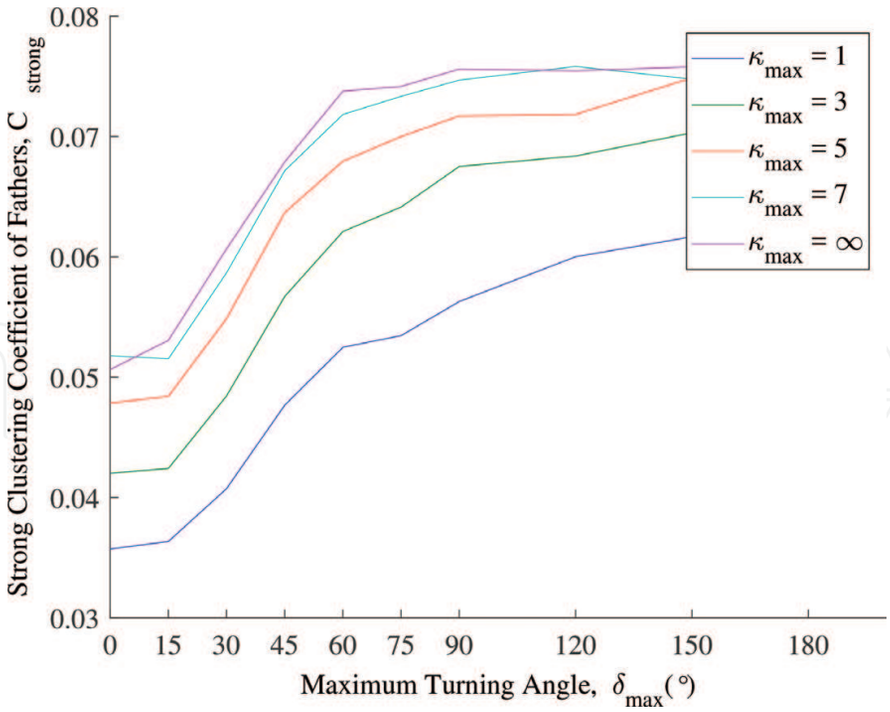

Figure 17. Strong clustering coefficient of fathers. Field size 133.2794 × 47.2927 units. Tree density $\omega = 0.071552$ trees per square unit ($\tau = 451$ Rice Center trees). Pollination chance diminishing with larger carryover. Maximum pollen carryover $\kappa_{max} = \{1, 3, 5, 7, \infty\}$.

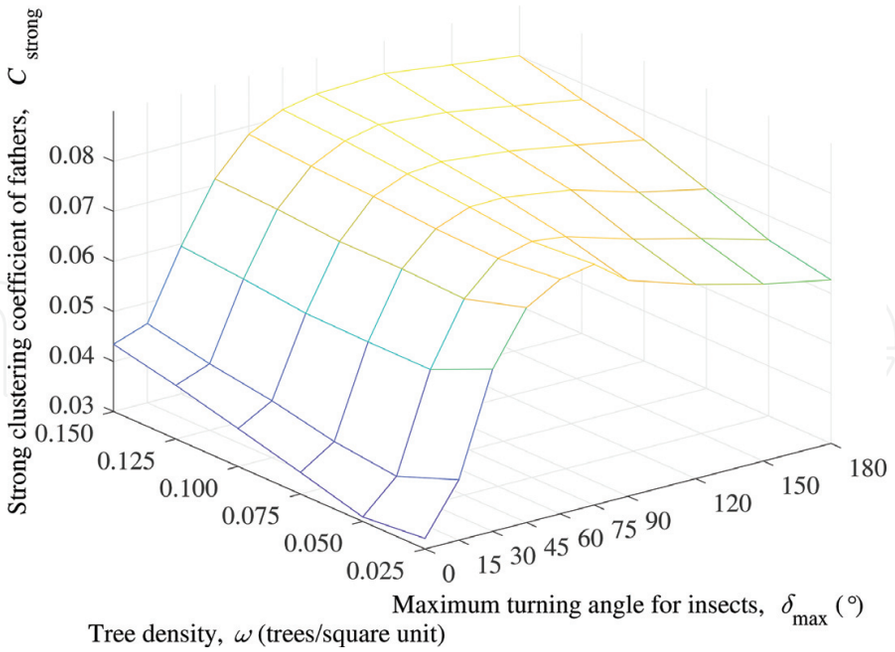

Figure 18. Strong clustering coefficient of fathers. Field size 100×100 units. Tree density in trees per square unit, $\omega = \{0.025, 0.050, 0.075, 0.100, 0.125, 0.150\}$ ($\tau = \{250, 500, 750, 1000, 1250, 1500\}$ randomly placed trees). Pollination chance diminishing with larger carryover. Maximum pollen carryover $\kappa_{\max} = \infty$.

4. Conclusions

From the agent-based, correlated random walk model presented, we observe the effects of varying the maximum pollen carryover, κ_{max}, the maximum pollinator turning area, $\delta_{\max}$, and the density of trees, ω, on the distribution of pollen within a population of *Cornus florida*.

When $\kappa_{\max}$ increases we see that the mean number of fathers per mother, the connectance, the average weighted diversity of fathers, the average and maximum average pollination distances, and the clustering coefficients all increase. The percentage increase varied between the measured, though the largest effect was seen in the connectance of the pollination graph. These increases are due to the increased capability of the pollinators to carry pollen farther from their source.

Changing the pollinator movement by increasing the maximum turning angle, $\delta_{\max}$, affected each of the measures as well. With most of the measures decreasing with increasing $\delta_{\max}$. These include the connectance, the average weighted diversity of fathers, and the average and maximum average pollination distances. On the other hand, the weak and strong clustering coefficients had maximal values between angles of 45 and 90°.

When $\delta_{\max} = 180°$, pollen is distributed in a purely random walk, and is more representative of pollen dispersal by wind. When $\delta_{\max} = 0°$, pollinators travel in a straight line, only changing direction when bouncing off of the boundary. This leads to a greater spatial displacement for each pollinator and thus a greater distance that pollen travels, resulting in greater genetic

diversity in the *C. florida* population. While neither of these extremes may be biologically relevant in *C. florida* populations, we note that the clustering coefficient of fathers, *C*, is maximized when δ_{max} is between 60 and 90°, which could help illuminate some of the biological processes at work in the system.

Major changes are observed when comparing simulations using randomly-placed trees with simulations using the tree-placement at the Rice Center. When using the Rice Center data, we see a bimodal distribution in the number of fathers per mother, the connectance values are halved, the average weighted diversity of fathers is lower, the average pollination distance is lower when δ_{max} is close to 0° and higher when δ_{max} is close to 180°, and the clustering coefficient of fathers exhibits both quantitative and qualitative differences. All of these differences highlight the need for specificity in describing the tree locations within a specific ecosystem in order to truly understand how pollen is distributed within that ecosystem. The differences in these graph indicators is due to the non-uniform distribution of trees at the Rice Center.

Funding

The collection of data and construction of an initial model were supported by a National Science Foundation grant (DEB-0640803) to Rodney J. Dyer and David M. Chan. James H. Lee was supported by a grant from the VCU Rice Center to complete an advance model. This manuscript is VCU Rice Center Manuscript #69.

Author details

James H. Lee[1], David M. Chan[1]* and Rodney J. Dyer[2]

*Address all correspondence to: dmchan@vcu.edu

1 Department of Mathematics and Applied Mathematics, Virginia Commonwealth University, Richmond, Virginia, USA

2 Center for Environmental Studies, Virginia Commonwealth University, Richmond, Virginia, USA

References

[1] Slatkin M. Gene flow in natural populations. Annual Review of Ecology and Systematics. 1985;**16**:393-430

[2] Morris WF. Predicting the consequence of plant spacing and biased movement for pollen dispersal by honey bees. Ecology. 1993;**74**:493-500

[3] Waples R, Gaggiotti O. What is a population? An empirical evaluation of some genetic methods for identifying the number of gene pools and their degree of connectivity. Molecular Ecology;**15**:1419-1438

[4] R. Dyer landscape and plant population genetics. In: Balkenhol N, Cushman S, Storfer A, editors. Landscape Genetics: Concepts, Methods, and Applications. John Wiley and Sons; 2015

[5] Levin D, Kerster H. Gene flow in seed plants. Evolutionary Biology;**7**:139-220

[6] Dyer R, RJ VS. Pollen pool heterogeneity in shortleaf pine, *Pinus echinata* mill. Molecular Ecology. 2001;**10**:859-866

[7] Manel S, Schwartz MK, Luikart G, Taberlet P. Landscape genetics: Combining landscape ecology and population genetics. Trends in Ecology & Evolution. 2003;**18**:189-197

[8] Dyer R. Is there such a thing as landscape genetics? Molecular Ecology. 2015;**24**:3518-3528

[9] Brunet J, Holmquist KGA. The influence of distinct pollinators on female and male reproductive success in the Rocky Mountain columbine. Molecular Ecology. 2009;**18**:3745-3758

[10] Foster E, Chan DM, Dyer RJ. Model comparison for abiotic versus biotic pollen dispersal. Nonlinear Dynamics, Psychology, and Life Sciences. (20):471-484

[11] Dyer RJ, Chan DM, Gardiakos VA, Meadows CA. Pollination networks: Quantifying pollen pool covariance networks and the influence of intervening landscape on genetic connectivity in the North American understory tree, *Cornus florida* L. Landscape Ecology. 2012;**27**:239-251

[12] DiLeo MF, Siu JC, Rhodes MK, López-Villalobos A, Redwine A, Ksiazek K, Dyer RJ. RJ. The gravity of pollination: Integrating at-site features into spatial analyses of contemporary pollen movement. Molecular Ecology. 2014;**23**:3793-3982

[13] R. J. Dyer, Coordinates of *C. florida* at the VCU Rice Center, (2014) . Unpublished

[14] Bartumeus F, Catalan J, Viswanathan GM, Raposo EP, da Luz MGE. The influence of turning angles on the success of non-oriented animal searches. Journal of Theoretical Biology. 2008;**252**:43-55

[15] Bovet P, Benhamou S. Spatial analysis of animal's movements using a correlated random walk model. Journal of Theoretical Biology. 1988;**131**:419-433

[16] Byers JA. Correlated random walk equations of animal dispersal resolved by simulation. Ecology. 2008;**82**:1620-1690

[17] Codling EA, Plank MJ, Benhamou S. Random walk models in biology. Journal of The Royal Society Interface. 2008;**5**:813-834

[18] Prasad BRG, Borges RM. Searching on patch networks using correlated random walks: Space usage and optimal foraging predictions using Markov chain models. Journal of Theoretical Biology. 2006;**240**:241-249

[19] Johnson SD, Nilsson LA. Pollen carryover, geitonogamy, and the evolution of deceptive pollination systems in orchids. Ecology. 1999;**80**:2607-2619

[20] deJong TJ, Klinkhamer PGL, Van Staalduinen MJ. The consequences of pollination biology for selection of mass or extended blooming. Functional Ecology. 1992;**6**:606-615

[21] Foster E. An agent based gene flow model [VCU Thesis and Dissertations]. 2009. Paper No. 1726

[22] Ramos-Jiliberto R, Albornoz AA, Valdovinos FS, Smith-Ramiriz C, Arim M, Armesto JJ, Marquet PA. A network analysis of plant-pollinator interaction in temperate rain forests of Chiloe, Chile. Oecologia. 2009;**160**:697-706

[23] Valdovinos FS, Ramos-Jiliberto R, Flores JD, Espinoza C, Lopez G. Structure and dynamics of pollination networks: The role of alien plants. Oikos. 2009;**118**:1190-1200

[24] Jørgensen SE. Ecosystem Ecology. Amsterdam, The Netherlands: Elsevier; 2009

[25] Traveset A, Chamorro S, Olesen JM, Heleno R. Space, time and aliens: Charting the dynamic structure of Galapagos pollination networks. AoB PLANTS 7: plv068. DOI: 10.1093/aobpla/plv068

[26] Lundgren R, Olesen JM. The dense and highly connected world of Greenland's plants and their pollinators. Arctic, Antarctic, and Alpine Research. 2005;**37**(4):514-520

[27] Borsch J, Gonzalez AMM, Rodrigo A, Navarro D. Plant-pollinator networks: Adding the pollinator's perspective. Ecology Letters. 2009;**12**:409-419

[28] Ferrero V, Castro S, Costa J, Acuna P, Navarro L, Loureiro J. Effect of invader removal: Pollinators stay but some native plants miss their new friend. Biological Invasions. 2013; **15**:2347-2358

[29] Bidaux R, Boccara N. Correlated random walks with a finite memory range. International Journal of Modern Physics C: Computational Physics and Physical Computation. 2000;**11**: 921-947

IntechOpen